Mansoura Engineering Journal

Volume 36 | Issue 1 Article 8

11-11-2020

Stress Distributions for T-Section Beams made of Functionally Graded Material.

Abla El-Megharbel
Production Engineering Department., Faculty of Engineering., Port-Said University., Port-Said 42523., Egypt.

Follow this and additional works at: https://mej.researchcommons.org/home

Recommended Citation
El-Megharbel, Abla (2020) "Stress Distributions for T-Section Beams made of Functionally Graded Material.," *Mansoura Engineering Journal*: Vol. 36 : Iss. 1 , Article 8.
Available at: https://doi.org/10.21608/bfemu.2020.122679

This Original Study is brought to you for free and open access by Mansoura Engineering Journal. It has been accepted for inclusion in Mansoura Engineering Journal by an authorized editor of Mansoura Engineering Journal. For more information, please contact mej@mans.edu.eg.

Stress distributions for T-section beams made of functionally graded material

Abla El-Megharbel
Port-Said University, Faculty of Engineering, Prod. Eng.&Mech. Des. Dept. Port-Said 42523, Egypt

توزيع الاجهادات على عارضة لها مقطع (T) و من مواد متدرجة الخواص الميكانيكية

خلاصة البحث

يهتم هذا البحث بدراسة الإجهادات الواقعة على عارضة لها مقطع (T) و من مواد متدرجة الخواص الميكانيكية (FGMs) وذلك خلال دراسة تحليلية في صورة معادلات رياضية. لذلك أهتم البحث بدراسة الإجهاد العمودي على العارضة و ذلك تحت تأثير حمل محوري و عزوم انحناء مع استخدام المحور الأساسي الفعال خلال البحث. و تم اعتبار معامل المرونة (E) متغيرا في هذه الدراسة في الإتجاه الرأسي و كذلك في الإتجاه العرضي و ذلك من خلال دالة أسية. كما أهتم البحث بدراسة معامل عدم التجانس على توزيع الإجهاد العمودي و كذلك موضع محور التعادل بالنسبة لإرتفاع العارضة. وأظهرت نتائج البحث التأثير الواضح لمعامل عدم التجانس على الإجهاد العمودي و كذلك على موضع محور التعادل لعارضة من مواد متدرجة الخواص الميكانيكية (FGMs). حيث أنه بزيادة القيمة المطلقة لمعامل عدم التجانس فإن الإجهاد العمودي للمنطقة الأقل صلابة في المقطع الهندسي يقل بينما الإجهاد العمودي في المنطقة الأكثر صلابة يزداد كما يتحرك موضع محور التعادل إلى اتجاه المنطقة الأكثر صلابة.

Abstract:

This study introduces a theoretical analysis for functionally graded materials (FGMs) of T-section beams. Analytical methods are set in the form of equations using the effective principal axes, in order to provide a method for predicting the normal stress distribution of the FGMs beam under both axial load and bending moments. Considering the elastic modulus to be an exponential function, the effect of the non-homogeneity parameter on the distribution of the normal stress, as well as on the position of the neutral axis along the beam height, is discussed for several different loading cases. The results obtained show that the non-homogeneity parameters have great effects on the normal stress distribution and on the position of the neutral axis. This indicates that, with the increase of the absolute value of the non-homogeneity parameter, the normal stress at the less hard region in the cross section decreases. Moreover, the normal stress at the harder region increases, and the neutral axis transfers toward the harder region.

Keywords Bending Moment, Functionally Graded Materials, Neutral Axis, Normal Stress, T-section Beam

1. Introduction

Functionally graded materials (FGMs) have been widely used in modern industries including aviation, aerospace, mechanical, transportation, energy, electronic, chemical, biomedical and civil engineering. The functionally graded materials (FGMs) are a class of advanced composites characterized by the gradual variation in composition, microstructure and material properties.

Many researches have been carried out to study the mechanical analysis of the FGMs components. Li et al., [1] have studied the mechanical model for rectangular FGMs under axial load and bending moments simplifying the assumption for the principal axes. While El Megharbel et al., [2] have studied the FGM beam with I-section under axial load and one bending moment. At present, some researches are interested in studying the T-section beams especially with FGMs.

Accepted March 30, 2011.

The study of the functionally graded material (FGM) has already been tackled by many investigators (Li et al., [1]; Zhen-yi, [3]; Ozturk and Erdogan, [4]).

Wang et al. [5] have analytically investigated the axisymmetric bending of circular plates whose material properties vary along the thickness. The transverse loads are expanded in terms of the Fourier–Bessel series, and the solutions corresponding to each item of the series are derived by a semi-inverse method.

In : thermal problems, An elastic–plastic stress analysis of FGM plates under a transient thermal loading cycle, which consists of heating followed by cooling, was carried out by Nemat-Alla et al. [6]. Whereas, the mechanical and thermal stresses in a functionally graded rotating disk with variable thickness due to radially symmetry loads were discussed by Bayat et al. [7].

The elastostatic problem of a hollow non-homogeneous cylindrical tube under internal loading have been analytically considered by Theotokoglou and Stampouloglou [8]. The static and kinematic shakedown of a plate made of functionally graded materials (FGMs) was analyzed by Peng et al. [9]. While Tung et al. [10] have investigated the stability of FG plates under in-plane compressive, thermal and combined loads. Material properties were assumed to be temperature-independent, and graded in the thickness direction according to a simple power law distribution. Equilibrium and compatibility equations for FG plates were derived using the classical plate theory. The resulting equations are solved by Galerkin procedure.

Li et al. [11] have studied the transient response of FGMs with a finite crack under anti-plane shear impact. Moreover, the anti-plane impact fracture analysis was performed for a weak-discontinuous interface in a symmetrical functionally graded composite strip by Li and Lee [12]. Carrera et al. [13] have evaluated the effect of thickness stretching in plate/shell structures made by materials which are functionally graded (FGM) in the thickness direction. This was achieved by removing the transverse normal strain in the kinematic assumptions of various refined plate/shell theories.

Ozturk and Erdogan [4] have calculated the stress intensity factors as functions of the non-homogeneity parameter for various loading conditions. The anti-plane fracture analysis, for a functionally graded coating–substrate system, with a crack inclined to the weak/micro-discontinuous interface, was performed by Li and Lee [14].

The stress distribution in rotating two composite structures of functionally graded solid disks was discussed by Zencour [15].

The mechanical property graded of the examined material, such as the elastic modulus or the shear modulus in the pervious studies, is set to be some certain function such as a linear function, a power function, an exponential function or even a hyperbolic function. .

The most widely-used component in engineering is the beam, for whose mechanical behaviour has an important significance for studying. Thus, the aim of this paper is to present a theoretical analysis for the FGMs of T-section beams under axial load and bending moments to determine the effect of the non-homogeneity parameter on the normal stress distributions.

2. Theoretical Analyses

The mechanical model of the FGMs beam, of the T-section considered in this study is shown in Fig. 1. In which H, B, h and b are the height and width of the T-section and the thickness of the flange and web of the section, respectively. The beam is subjected to an axial load N_x and two bending moments M_y and M_z. The elastic modulus is assumed to vary continuously in the two directions: the height and the width directions. Thus the elastic non-homogeneity, in the fixed coordinate system OXYZ (Fig. 1), is assumed to be in the following exponential form, Konda and Erdogan [16]

$$E(Y,Z) = E_o e^{\beta_1 Y + \beta_2 Z} \quad (1)$$

where E_0 is the elastic modulus at the origin point O; β_1 and β_2 are the non-homogeneity parameters in Y and Z directions respectively.

For the above-mentioned FGM beam, the traditional centroidal principal axes are no longer suitable for the analysis of the normal stress. The following analysis is based on the effective principal axes through a new coordinate system *oxyz* (see Fig. 1) with the point o(0, $\alpha_1 H$, $\alpha_2 B$) in OXYZ as a new origin where

$$y = Y - \alpha_1 H \quad \text{and} \quad z = Z - \alpha_2 B \quad (2)$$

are the effective principal axes, whereas (α_1) and (α_2) are the position parameters of the effective principal axes *z* and *y* respectively. The values of the parameters (α_1) and (α_2) are related to the non-homogenous parameters β_1 and β_2 which will be determined later on. In the new coordinate system *oxyz*, the elastic modulus of the beam may be expressed as follows:

$$E(y,z) = E_1 e^{\beta_1 y + \beta_2 z} \quad (3)$$

where E_1 is the elastic modulus at the point o(0, $\alpha_1 H$, $\alpha_2 B$) and may be expressed as

$$E_1 = E_o e^{\alpha_1 \beta_1 H + \alpha_1 \beta_2 B} \quad (4)$$

The normal stress, in the x direction, acting on the FGM beam may be expressed as:

$$\sigma_x = E_1 e^{\beta_1 y + \beta_2 z} \varepsilon_x \quad (5)$$

The beam is assumed to be stressed by an axial load (N_x) as well as the bending moments M_y and M_z at the same time as shown in Fig. 1. Assuming the linear strain produced by the axial force are the same for the different points in the cross section. Moreover, the curvatures produced by the bending moments are also identical. Therefore, the equation of compatibility for the beam is expressed as follows:

$$\varepsilon_x = \varepsilon_o - \frac{y}{\rho_z} + \frac{z}{\rho_y} \quad (6)$$

The previous equation assumed that the beam is loaded by the axial force and the bending moment simultaneously. ε_o is the homogenous axial linear strain in the cross section, ρ_z and ρ_y are the radii of curvature in the vertical and horizontal plane of the beam, respectively.

Assuming that:

$$\int_{b_4}^{b_3}\int_{h_2}^{h_1} y e^{\beta_1 y} e^{\beta_2 z} dydz + \int_{b_5}^{b_6}\int_{h_1}^{h_3} y e^{\beta_1 y} e^{\beta_2 z} dydz = 0 \quad (7)$$

$$\int_{b_4}^{b_3}\int_{h_2}^{h_1} z e^{\beta_1 y} e^{\beta_2 z} dydz + \int_{b_5}^{b_6}\int_{h_1}^{h_3} z e^{\beta_1 y} e^{\beta_2 z} dydz = 0 \quad (8)$$

(which are more accurate than the assumption in Li [1])

Where the beam geometry constants are:

$$b_1 = \left(\frac{B+b}{2}\right), \quad b_2 = \left(\frac{B-b}{2}\right),$$

$$b_3 = b_1 - \alpha_2 B, \quad b_4 = b_2 - \alpha_2 B,$$

$$b_5 = b_3 - b_1, \qquad b_5 = b_2 + b_3 \tag{9}$$

$$h_1 = H - \alpha_1 H - h, \qquad h_2 = -\alpha_1 H,$$

$$h_3 = h_1 + h$$

Therefore, the position parameters α_1 and α_2 of the effective principal axes z and y may be expressed, from Eqs. (7-8), as

$$\alpha_1 = \frac{\{[(H-h)\beta_1 - 1]e^{(H-h)\beta_1} + 1\}k_1 + \{[H\beta_1 - 1]e^{H\beta_1} + [1-(H-h)\beta_1]e^{(H-h)\beta_1}\}k_2}{H\beta_1 k_3} \tag{10}$$

$$\alpha_2 = \frac{\{[b_1\beta_2 - 1]e^{b_1\beta_2} + [b_2\beta_2 + 1]e^{b_2\beta_2}\}k_4 + \{[B\beta_2 - 1]e^{B\beta_2} + 1\}k_5}{B\beta_2 k_3} \tag{11}$$

Where

$$k_1 = \left(e^{b_1\beta_2} - e^{b_2\beta_2}\right), \quad k_2 = \left(e^{B\beta_2} - 1\right)$$
$$k_3 = \left(e^{(H-h)\beta_1} - 1\right)k_1 + \left(e^{H\beta_1} - e^{(H-h)\beta_1}\right)k_2$$
$$k_4 = \left(e^{(H-h)\beta_1} - 1\right), \quad k_5 = \left(e^{H\beta_1} - e^{(H-h)\beta_1}\right) \tag{12}$$

According to Eqs. (10 and 11), it is found that when the beam is non-homogenous, along both y and z directions, the effective principal axes z and y are not the centroid axes. Whereas, when the beam is rectangular (b=B, h=H), the same formulae as in Li [1] apply for the position parameters α_1 and α_2.

Furthermore, the equilibrium equations of the above-mentioned beam, under axial load and bending moments, can be expressed as El Megharbel et al. [17]:

$$N_x = \int_A \sigma_x dA, \qquad -M_z = \int_A \sigma_x y dA,$$
$$M_y = \int_A \sigma_x z dA \tag{13}$$

Substituting in the previous equation with Eqs. (5-6), yields to:

$$N_x = E\int_{b_4}^{b_3}\int_{h_2}^{h_1}\left(\varepsilon_o - \frac{y}{\rho_z} + \frac{z}{\rho_y}\right)e^{\beta_1 y}e^{\beta_2 z}dydz + \int_{b_5}^{b_6}\int_{h_1}^{h_3}\left(\varepsilon_o - \frac{y}{\rho_z} + \frac{z}{\rho_y}\right)e^{\beta_1 y}e^{\beta_2 z}dydz = 0 \tag{14}$$

$$-M_z = E_1\int_{b_4}^{b_3}\int_{h_2}^{h_1}\left(\varepsilon_o y - \frac{y^2}{\rho_z} + \frac{yz}{\rho_y}\right)e^{\beta_1 y}e^{\beta_2 z}dydz + E_1\int_{b_5}^{b_6}\int_{h_1}^{h_3}\left(\varepsilon_o y - \frac{y^2}{\rho_z} + \frac{yz}{\rho_y}\right)e^{\beta_1 y}e^{\beta_2 z}dydz = 0 \tag{15}$$

$$M_y = E_1\int_{b_4}^{b_3}\int_{h_2}^{h_1}\left(\varepsilon_o z - \frac{yz}{\rho_z} + \frac{z^2}{\rho_y}\right)e^{\beta_1 y}e^{\beta_2 z}dydz + E_1\int_{b_5}^{b_6}\int_{h_1}^{h_3}\left(\varepsilon_o z - \frac{yz}{\rho_z} + \frac{z^2}{\rho_y}\right)e^{\beta_1 y}e^{\beta_2 z}dydz = 0 \tag{16}$$

Applying Eqs. (7-8) into Eqs. (14-16) the following can be obtained

$$\varepsilon_o = \frac{N_x}{E_1 A^*} \tag{17}$$

$$E_1\left(-\frac{k_7}{\rho_z} + \frac{k_8}{\rho_y}\right) = -M_z \tag{18}$$

$$E_1\left(-\frac{k_8}{\rho_z} + \frac{k_{11}}{\rho_y}\right) = M_y \tag{19}$$

Where:

$$A^* = \frac{k_3}{\beta_1\beta_2 k_6} \tag{20}$$

$$k_6 = e^{\alpha_1 H\beta_1}\cdot e^{\alpha_1 B\beta_2} \tag{21}$$

$$k_7 = \frac{\{a_1 e^{(H-h)\beta_1} - a_2\}k_1 + \{a_3 e^{H\beta_1} - a_4 e^{(H-h)\beta_1}\}k_2}{\beta_2\beta_1^3 k_6} \tag{22}$$

$$k_8 = \frac{\{a_9 e^{b_1\beta_2} - a_{10}e^{b_2\beta_2}\}\cdot k_9 + \{a_{11}e^{B\beta_2} + a_{12}\}k_{10}}{\beta_1^2\beta_2^2 k_6} \tag{23}$$

$$k_9 = (h_1\beta_1 - 1)e^{(H-h)\beta_1} + h_2\beta_1 + 1 \tag{24}$$

$$k_{10} = ((H-h_2)\beta_1 - 1)e^{H\beta_1} - (h_1\beta_1 - 1)e^{(H-h)\beta_1} \tag{25}$$

$$k_{11}=\frac{\left\{a_5e^{h_1\beta_1}-a_6e^{h_2\beta_1}\right\}\cdot k_4+\left\{a_7e^{H\beta_2}-a_8\right\}k_5}{\beta_1\beta_2^3k_6} \quad (26)$$

$$a_1=(h_1\beta_1-1)^2+1,$$
$$a_2=(h_2\beta_1+1)^2+1,$$
$$a_3=((H-h_2)\beta_1-1)^2+1$$
$$a_4=(h_1\beta_1-1)^2+1$$
$$a_5=(b_3\beta_2-1)^2+1$$
$$a_6=(b_4\beta_2-1)^2+1 \quad (27)$$
$$a_7=((1-\alpha_2)B\beta_2-1)^2+1$$
$$a_8=(\alpha_2B\beta_2+1)^2+1$$
$$a_9=b_3\beta_2-1$$
$$a_{10}=b_4\beta_2-1$$
$$a_{11}=(1-\alpha_2)B\beta_2-1$$
$$a_{12}=\alpha_2B\beta_2+1$$

According to (18) and (19):

$$\frac{1}{\rho_z}=-\frac{k_{11}M_z+k_8M_y}{E_1\left(k_8^2-k_7k_{11}\right)} \quad (28)$$

$$\frac{1}{\rho_y}=-\frac{k_7M_y+k_8M_z}{E_1\left(k_8^2-k_7k_{11}\right)} \quad (29)$$

Substituting in Eqs. (20, 28 and 29) with the rectangular beam condition (b=B, h=H), an agreement with Li [1] can be found in equation (20), and a complete disagreement in Eqs. (28 and 29). This disagreement in the late equations is due to the simplified assumption in Li [1] rather than the accurate assumption (Eqs. 7-8) in this paper.

The total normal stress in the beam in the x-direction may be obtained by the aid of Eqs. (5, 6, 17, 28, 29) as

$$\sigma_x=\sigma_x^I+\sigma_x^{II}+\sigma_x^{III} \quad (30)$$

Where σ_x^I is the normal stress due to the axial force N_x (Eq. 4, 17), while σ_x^{II} and σ_x^{III} are the normal stresses due to the bending moments in the vertical and horizontal plane of the beam (Eq. 4, 28, 29), respectively. Therefore it can be written in the following form:

$$\sigma_x^I=\frac{N_x}{E_1A^*}E_oe^{\beta_1Y+\beta_2Z} \quad (31)$$

$$\sigma_x^{II}=-\frac{k_{11}M_z+k_8M_y}{E_1\left(k_8^2-k_7k_{11}\right)}E_o\left(Y-\alpha_1H\right)e^{\beta_1Y+\beta_2Z} \quad (32)$$

Where σ_x^{II} is the normal stress related to ρ_z

$$\sigma_x^{III}=-\frac{k_7M_y+k_8M_z}{E_1\left(k_8^2-k_7k_{11}\right)}E_o\left(Z-\alpha_2B\right)e^{\beta_1Y+\beta_2Z} \quad (33)$$

Where σ_x^{III} is the normal stress related to ρ_y. Assume that $\sigma_x^I+\sigma_x^{II}+\sigma_x^{III}=0$ then the distance Y may be obtained as

$$Y=\left.\begin{array}{l}\dfrac{N_x\left(k_8^2-k_7k_{11}\right)}{A^*\left(k_{11}M_z+k_8M_y\right)}\\ -\dfrac{k_7M_y+k_8M_z}{k_{11}M_z+k_8M_y}\left(Z-\alpha_2B\right)+\alpha_1H\end{array}\right\} \quad (34)$$

3. Results and discussion

The mathematical models for the normal stress of FGMs for T-sections are introduced in the previous section. The effect of the non-homogeneity parameters (β_1 and β_2) on the distribution of the normal stress and on the position of the neutral axis is substantial. A schematic topology for the hard region and the less hard region for T-section FGM beam is illustrated in Fig. 2 The distribution of the normal stress along the height of the FGM beam (from Y=0 to Y=H, see Fig. 1) is illustrated in Figs. 3-10.

Taking a constant value for the non-homogeneity parameter (β_2) is a reasonable simplified way to detect the effect of the non-homogeneity parameter (β_1), which is almost the same effect of the other the non-homogeneity parameter (β_2). The values of the non-homogeneity parameter (β_1) is discussed from almost a zero value (0.05) to a very rigid value (β_1 =10). The effect of the absolute value of the non-homogeneity parameter (β_1) on the normal stress σ_x^I is illustrated in Figs. 3-4 with a constant value for (β_2). When the beam is loaded by the axial force N_x only, it was noticed that the normal stress σ_x^I in the less hard region of the cross section is much lower than that in the harder region. Whereas, with the increase of the absolute value of (β_1), the σ_x^I in the less hard region decreases, whereas, that in the harder region increases. Moreover the effect of the negative sign of (β_1) has a great effect on the magnitude of σ_x^I compared to the positive sign of (β_1) for the same beam constants.

The effect of the non-homogeneity parameter (β_1) on the normal stress σ_x^{II} distribution along the beam height is shown in Figs. 5&6, with a constant value for (β_2). The normal stress σ_x^{II} distribution is due to the curvature in the vertical plane, when the FGM beam is stressed by bending moments (M_z) and (M_y). As the absolute value of the non-homogeneity parameter (β_1) increases, the σ_x^{II} in the less hard region decreases, whereas, that in the harder region increases. Moreover the negative sign of (β_1) has a positive effect on the magnitude of σ_x^{II} compared to the positive sign of (β_1) for the same beam constants (this conclusion was expected due to the arrangement of (β_1) in the obtained equations).

Whereas the normal stress σ_x^{III} distribution along the beam height with the effect of the non-homogeneity parameter (β_1), with a constant value for (β_2) is shown in Figs. 7&8. The normal stress σ_x^{III} distribution is due to the curvature in the horizontal plane, when the FGMs beam is stressed by bending moments (M_z) and (M_y). As the absolute value of the non-homogeneity parameter (β_1) increases, the σ_x^{III} in the more rigid region of the cross section increases, however, that in the less rigid region decreases. Moreover, as shown above, the positive sign of (β_1) has a negative effect on the magnitude of σ_x^{III} compared to the negative sign of (β_1) for the same beam constants.

The effect of the non-homogeneity parameter (β_1) on the total normal stress σ_x distribution along the beam height is shown in Figs. 9-10, with a constant value for (β_2). These results correspond to the FGM T-beam stressed by axial load (N_x) and bending moments (M_z) and (M_y), simultaneously. The results demonstrate similar general trends between Figs. 5-9 for (β_1) >0 and Figs. 6-10 for (β_1) <0; except that the values are different due to the effect of the normal force (N_x).

From Figs. 9-10, it can be indicated that the value of (β_1) has almost no effect on the normal stress along the beam height (H) at two points (0.07, 0.47) for (β_1) <0 and (0.1, 0.5) for (β_1) >0. From Figs. 3-10 it can be concluded that if the absolute value of the non-homogeneity parameter (β_1) is 0.05, which is almost a zero value, the normal stress in the FGMs beam is varying straightly with the beam height (H), which means that the beam is related to a

homogenous material. As the non-homogeneity parameter (β_1) increases, the normal stress varies non-linearly along the beam height.

The effect of non-homogeneity parameter (β_1) on the position of the neutral axis along the beam height is displayed in Figs. 11-12 for FGMs beam under axial load and bending moments. As the absolute value of the non-homogeneity parameter (β_1) increases, the position of the neutral axis transfers towards the hard region.

4. Conclusion

The mechanical model is established for the functionally graded material (FGM) beam with T-cross section, and its agreement with a rectangular cross section (FGM) is discussed. The effect of the non-homogeneity parameters on the normal stress distribution along the beam height with different loading cases for the functionally graded material (FGM) for T-section beam was included. The beam was subjected to an axial load with two bending moments and it was assumed that the elastic modulus varies continuously, both in the height and the breadth directions, with exponential functions. The normal stress analysis of the bending beam for T-sections was carried in the coordinate system, consisting of the effective principal axes, rather than the centroidal principal axes.

The effect of the non-homogeneity parameters on the position of the neutral axis is also examined. The present work can provide a good reference for the design of the functionally graded materials of T-section beams in engineering application.

References

01 Li, Y.D., Zhang, H., Zhang, N., Dai, Y., Stress analysis of functionally graded beam using effective principal axes, Int. J. Mech. Mater. Des., pp. 157-164, 2005.

02 El Megharbel, A., Abd El-Hafez, H., Stress analysis of FGM for I-section beams, ERJ Engineering Research Journal Faculty of Engineering Minoufia University, vol. 32 (4), No. 4, pp. 551-557, 2009.

03 Zhen-yi, J., The general solution for axial symmetrical bending of nonhomogenous circular plates resting on an elastic foundation, Applied Mathematics and Mechanics 12 (9), pp. 871-879, 1991.

04 Ozturk, M., Erdogan, F., The axisymmetric crack problem in a nonhomogeneous medium, Lehigh University, Bethlehem, PA, Final Project Report, 1992.

05 Wang, Y., Xu, R. Q., Ding, H. J., Analytical solutions of functionally graded piezoelectric circular plates subjected to axisymmetric loads, Acta Mech 215, pp. 287–305, 2010.

06 Nemat-Alla, M., Ahmed, K., Hassab-Allah, I., Elastic–plastic analysis of two-dimensional functionally graded materials under thermal loading, International Journal of Solids and Structures 46, pp. 2774–2786, 2009.

07 Bayat, M., Saleem, M., Sahari, B.B., Hamouda, A.M.S., Mahdi, E., Mechanical and thermal stresses in a functionally graded rotating disk with variable thickness due to radially symmetry loads, International Journal of Pressure Vessels and Piping 86, pp. 357–372, 2009.

08 Theotokoglou, E.E., Stampouloglou, I.H., The radially nonhomogeneous elastic axisymmentric problem, International Journal of Solids and Structures 45, pp. 6535–6552, 2008.

09 Peng, X., Zheng, H., Hu, N., Fang, C., Static and kinematic shakedown analysis of FG plate subjected to constant mechanical load and cyclically varying temperature change, Composite Structures 91, pp. 212–221, 2009.
10 Tung. H. V., Duc, N. D., Nonlinear analysis of stability for functionally graded plates under mechanical and thermal loads, Composite Structures 92, pp. 1184–1191, 2010.
11 Li, C., Weng, G.J., Z. Duan, Z., Zou, Z., Dynamic stress intensity factor of a functionally graded material under antiplane shear loading, Acta Mechanica 149, pp. 1-10, 2001.
12 Li, Y.D., Lee, K.Y., Fracture analysis of a weak-discontinuous interface in a symmetrical functionally graded composite strip loaded by anti-plane impact, Arch. Appl. Mech. 78, pp. 855–866, 2008.
13 Carrera, E., Brischetto, S., Cinefra, M., Soave, M., Effects of thickness stretching in functionally graded plates and shells, Composites: Part B, under press, 2010.
14 Li, Y.D., Lee, K.Y., Effects of the weak/micro-discontinuity of interface on the fracture behavior of a functionally graded coating with an inclined crack, Arch. Appl. Mech., 2008.
15 Zenkour , A.M., Stress distribution in rotating composite structures of functionally graded solid disks, J. Mater. Process. Technol. 209, pp. 3511–3517, 2009.
16 Konda, N., Erdogan, F., The mixed-mode crack problem in a nonhomogeneous elastic medium, Engng. Fract. Mech. 47(3), pp. 533–545, 1994.
17 El Megharbel, A., El Nasser, G.A., El Domiaty, A., Bending of tube and section made of strain-hardening material, J. Mater. Process. Technol. 203, pp. 372–380, 2008.

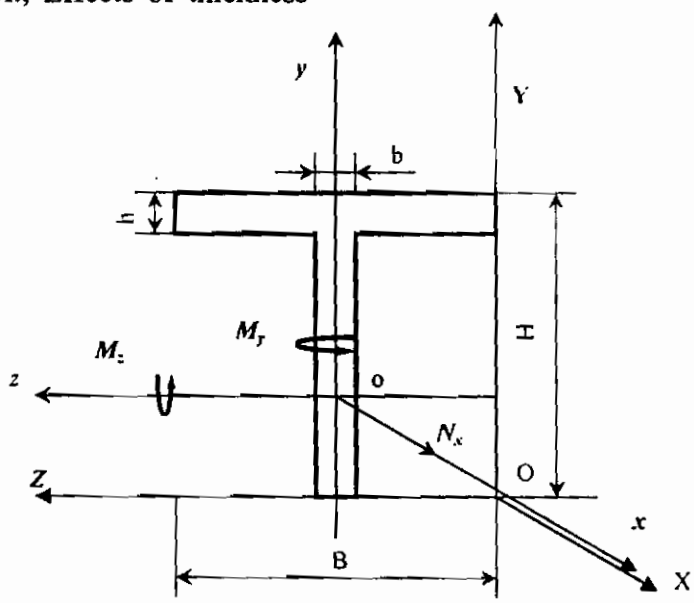

Fig. 1 The mechanical model of the bi-directional T-section FGM beam

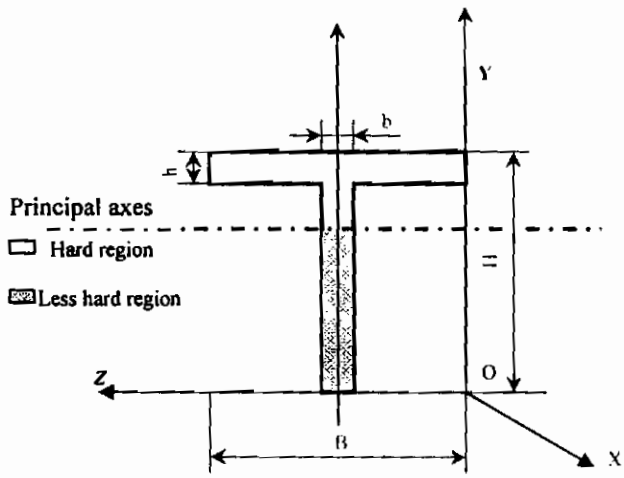

Fig. 2 A schematic topology for the hard region and the less hard region for T-section FGM beam

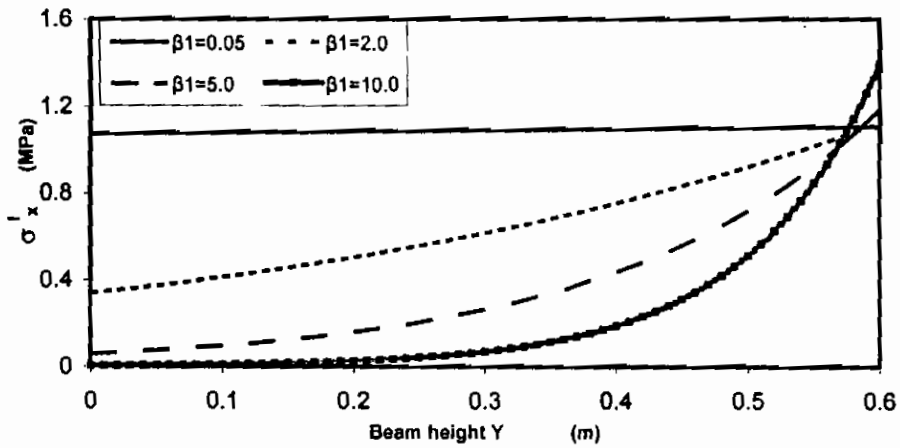

Fig. 3 The σ_x^I distributions along the FGM beam height (Y) with different (β_1) values (H=0.6m, B=0.3m, h=0.12m, b=0.06m, β_2= 10, N_x=20kN, M_z=M_y =0)

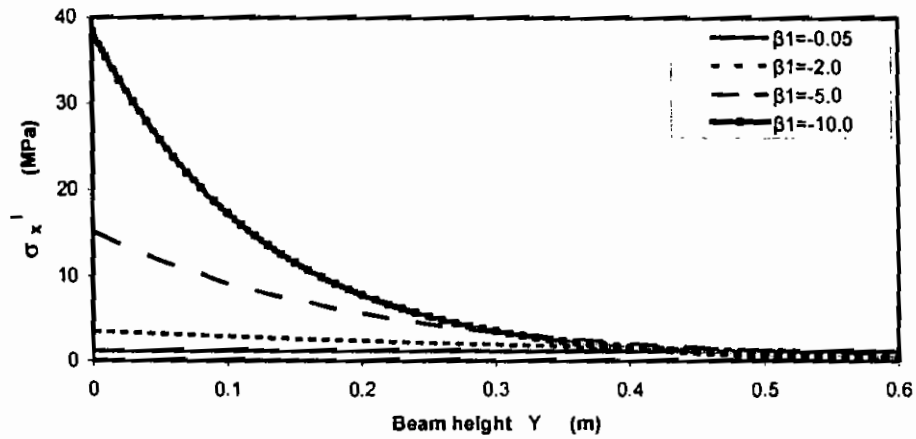

Fig. 4 The σ_x^I distributions along the FGM beam height (Y) with different (β_1) values (H=0.6m, B=0.3m, h=0.12m, b=0.06m, β_2= 10, N_x=20kN, M_z=M_y =0)

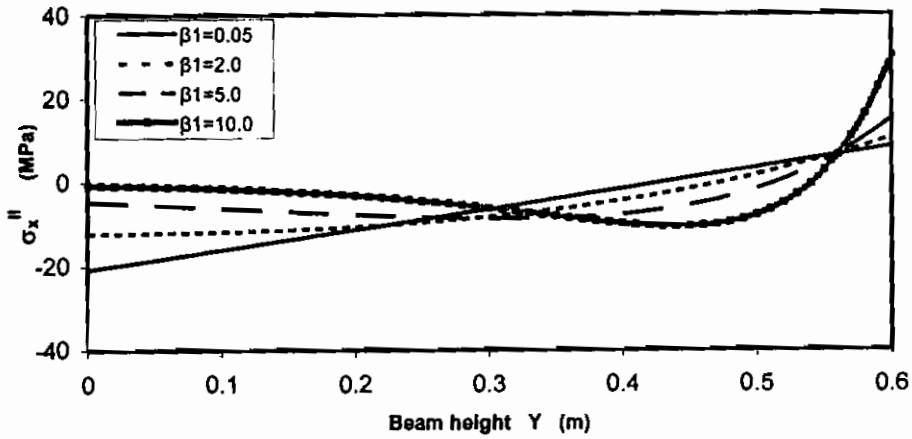

Fig. 5 The σ_x^{II} distributions along the FGM beam height (Y) with different (β_1) values (H=0.6m, B=0.3m, h=0.12m, b=0.06m, β_2= 10, N_x=0, M_z=M_y =20kN.m)

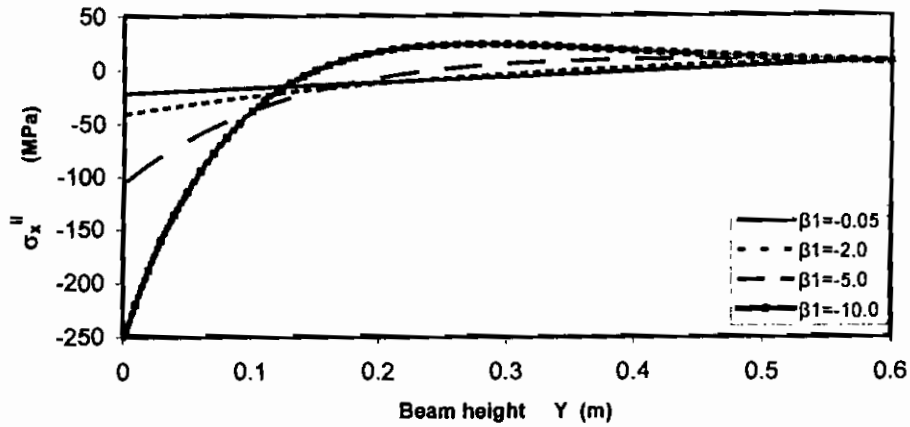

Fig. 6 The σ_x^{II} distributions along the FGM beam height (Y) with different (β_1) values (H=0.6m, B=0.3m, h=0.12m, b=0.06m, β_2= 10, N_x=0, M_z=M_y =20kN.m)

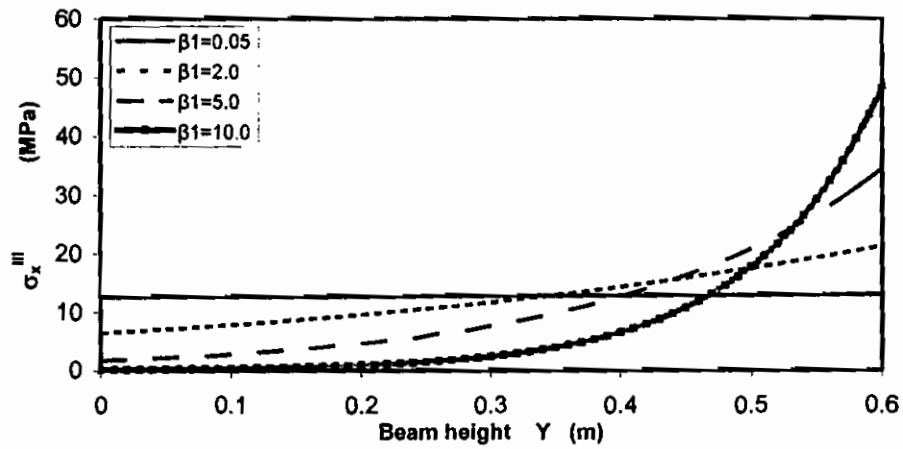

Fig. 7 The σ_x^{III} distributions along the FGM beam height (Y) with different (β_1) values (H=0.6m, B=0.3m, h=0.12m, b=0.06m, β_2= 10, N_x=0, M_z=M_y =20kN.m)

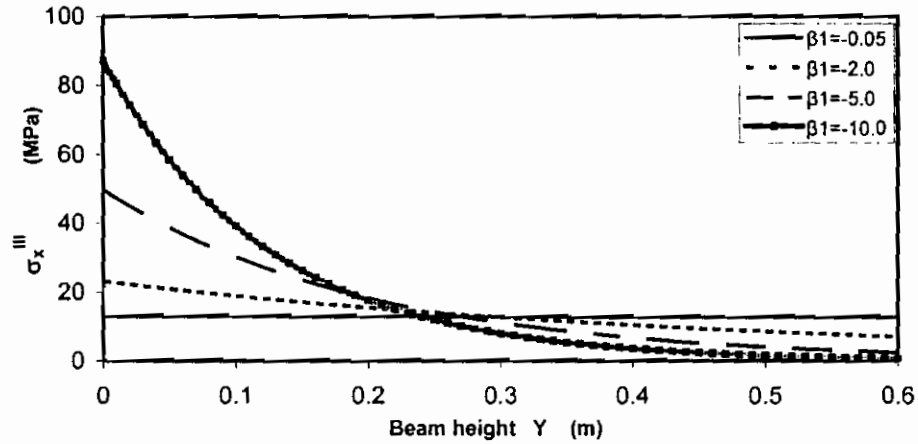

Fig. 8 The σ_x^{III} distributions along the FGM beam height (Y) with different (β_1) values (H=0.6m, B=0.3m, h=0.12m, b=0.06m, β_2= 10, N_x=0, M_z=M_y =20kN.m)

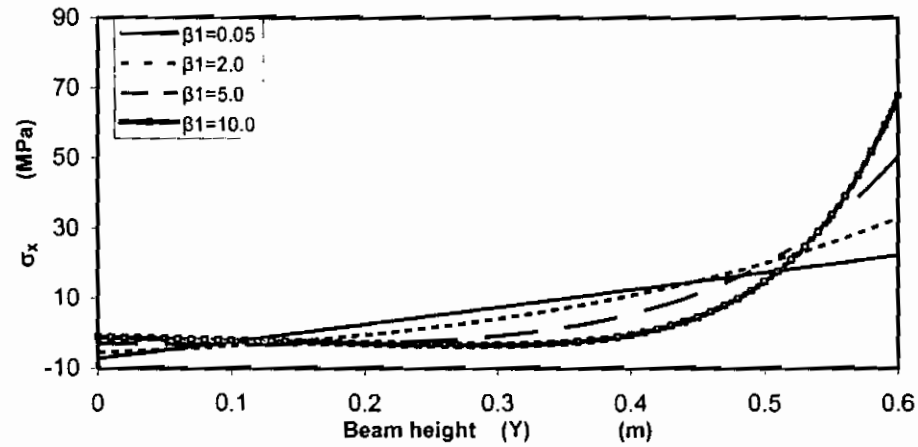

Fig. 9 The σ_x distributions along the FGM beam height (Y) with different (β_1) values (H=0.6m, B=0.3m, h=0.12m, b=0.06m, β_2= 10, N_x=20kN, M_z=M_y =20kN.m)

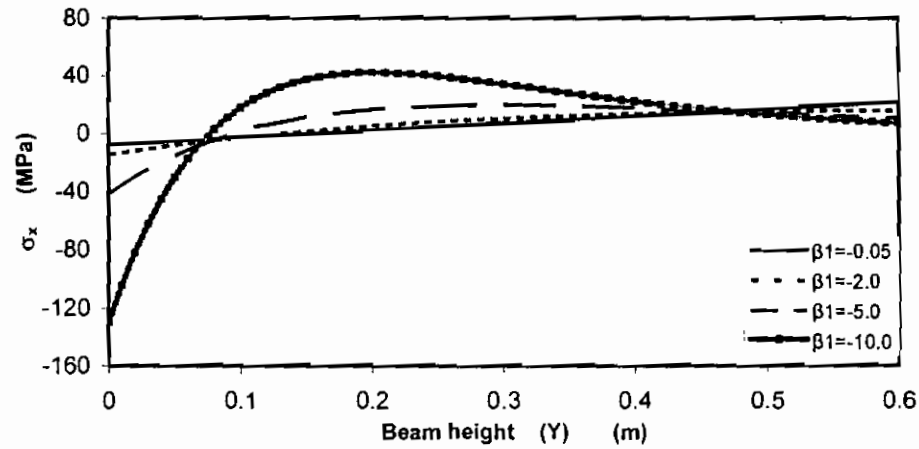

Fig. 10 The σ_x distributions along the FGM beam height (Y) with different (β_1) values (H=0.6m, B=0.3m, h=0.12m, b=0.06m, β_2= 10, N_x=20kN, M_z=M_y =20kN.m)

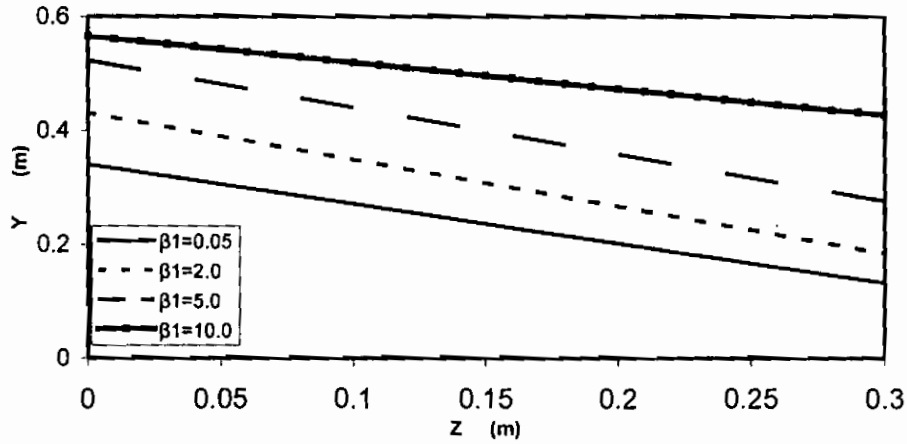

Fig. 11 The position of neutral axis in the cross section of the FGM beam with different (β_1) values (H=0.6m, B=0.3m, h=0.12m, b=0.06m, β_2= 10, N_x=20kN, M_z=M_y =20kN.m)

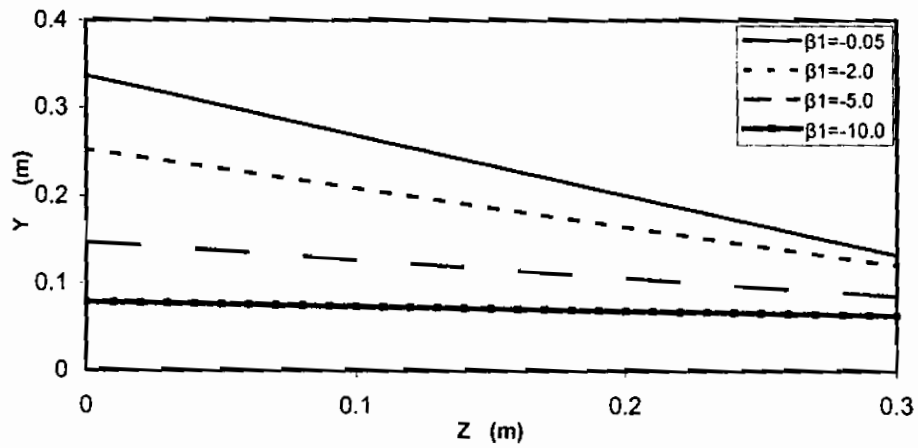

Fig. 12 The position of neutral axis in the cross section of the FGM beam with different (β_1) values (H=0.6m, B=0.3m, h=0.12m, b=0.06m, β_2= 10, N_x=20kN, M_z=M_y =20kN.m)